J. Astrophys. Astr. (1992) **13,** 293–305

VRI Photometry of M67 for CCD Standardization at 2.3m VBT

P. N. Bhat & K. P. Singh *Tata Institute of Fundamental Research, Bombay 400 005*
T. P. Prabhu *Indian Institute of Astrophysics, Bangalore 560 034*
A. K. Kembhavi *Inter University Centre for Astronomy & Astrophysics, Pune 410 007*

Received 1992 September 15; accepted 1992 November 16

Abstract. We present the results from CCD photometry in the *V, R* and *I* bands, of the 'Dipper Asterism' region of the open cluster M67 based on observations carried out at the prime focus of the 2.3 m Vainu Bappu Telescope of the Vainu Bappu Observatory, Kavalur. The CCD parameters like the system gain and the readout noise are measured using several flatfield frames taken through the standard *I* filter. The CCD chip is calibrated using the photometric standards in the field and linear colour transformation relations are derived. Also a few new *VRI* photometric measurements are reported for the members of the cluster.

Key words: Open clusters, M67—photometry—CCD calibration

1. Introduction

The use of a Charge Coupled Device (CCD) for optical photometry in astronomy allows a simultaneous definition of external variables such as the seeing, the sky brightness, and star positions on the detector along with the measurement of apparent intensities of an ensemble of stars. This involves the measurement of the photometric response of the detector which leads to a set of transformation equations to convert the Analog to Digital Units (ADU or sometimes called as Digital Numbers, DN) read from the CCD to apparent magnitudes. To calibrate the photometric response of a CCD, it is ideal to observe standard stars in a cluster having similar visual magnitudes and possessing as broad a spread in their colour indices as possible. M67 (NGC 2682) is an ideal open cluster for this purpose for the following reasons:

(i) In a small region covered by a single CCD frame it contains stars with a wide range of colours;
(ii) many of the stars are of similar brightness (V = 10 – 12), but very faint ($m_v \sim 20$) and very bright ($m_v \sim 9.7$) stars are also available in the same cluster;
(iii) the cluster is at a high galactic latitude (l = 216°, b = 32°) and the background stars do not interfere with the brightness measurements; and
(iv) it is an open cluster where individual stars can be easily resolved. The 'dipper asterism' region of the cluster is at $\alpha_{1950} = 8^h48^m36^s.6$ and $\delta_{1950} = +\ 11°57'33''$ which is easily accessible from the Vainu Bappu Observatory (VBO), Kavalur ($\lambda = +\ 12°34'.58$ and $l = -\ 78°49'.58$).

The exposures required on a 2.34 m Vainu Bappu Telescope (VBT), Kavalur, using

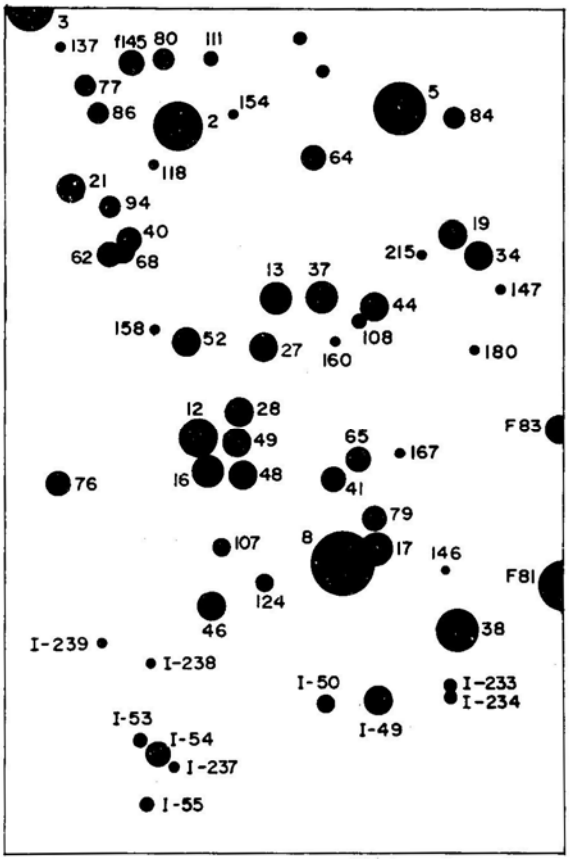

Figure 1. Finding chart of the CCD field of M67 centred around the 'dipper asterism'. The identifications follow Gilliland *et al.* (1991), Racine (1971) and Eggen & Sandage (1964). The whole field is about 6 arcmin × 4 arcmin. North is to the top and east is towards the left.

the CCD at its prime focus, were in the range 10–300s for *V, R* and *I* broadband filters. Fig. 1 is a finding chart of the region of M67 covered in our observations, centred around the 'dipper asterism' region. The stars are numbered following Gilliland *et al.* (1991) and Racine (1971). Previous photometric measurements of this cluster available in the literature are by Johnson & Sandage (1955); Eggen & Sandage (1964); Schild (1983, 1985) and more recently by Ram Sagar & Pati (1990); Joner & Taylor (1990); Chevalier & Ilovaisky (1991) and Mayya (1991). Time-resolved CCD photometry of the core region of M67 has recently been carried out by Gilliland *et al.* (1991)

In this paper we present the results from observations of M67 cluster using *VRI* broadband filters. The data from these observations are used to calibrate the CCD and also to obtain new photometric measurements. We have also used the flatfield images to derive CCD parameters like the readout noise, the system gain and the spatial noise component. The paper is organized as follows: In section 2 we describe the observations followed by data analysis and results in section 3. The conclusions are presented in section 4.

Table 1. Summary of filter characteristics.

Filter	Central wavelength (A)	Bandwidth (A)
I	8150	1700
R	6550	1300
V	5425	1050

Table 2. Summary of exposures through different broadband filters.

Date	Filter	Hour angle h m s	Air mass X	Sky brightness (mag/arcsec)	PSF FWHM (Pixels)	Exposure (*s*)
27.1.1990	*R*	0 53 44	1.024	20.13	6.5	10
27.1.1990	*R*	0 56 5	1.027		6.5	60
27.1.1990	*R*	1 0 31	1.035		6.5	300
28.1.1990	*V*	0 20 35	1.0034	21.87	6.0	20
28.1.1990	*V*	0 40 38	1.0147		5.8	120
28.1.1990	*I*	1 43 0	1.1004	19.16	5.8	10
28.1.1990	*I*	1 46 49	1.110		5.8	60
28.1.1990	*I*	1 50 50	1.124		5.6	300

2. Observations

The data acquisition system for the TIFR CCD is based on a GEC P8603/B (B-grade with a few bad columns) front illuminated chip which was commissioned sometime back (Bhat *et al.* 1990). The details of filters used for *VRI* photometry are summarized in Table 1. The observations were carried out during 1990 January 27–28, at the prime focus of VBT. The CCD consists of 576 × 385 pixels each of size 22 μm. This pixel size corresponds to a plate scale of 0.6 arcsec per pixel at the *F*/3.25 prime focus of VBT, at an image scale of 4.5 arcmin per cm. The total field of the CCD is 5.7 × 3.8 arcmin. Only one filter could be used per night since remote control of the filter wheel was not yet operational. A minimum of three frames of the dipper asterism were obtained with three different exposures in order to detect the faintest stars ($m_v \sim 20$) with a good statistical accuracy. The full width half maximum (FWHM) of the point spread function was $\simeq$ 3.0 arcsec. The sky brightness and the seeing were reasonably steady during these two observing nights. The cluster was close to the zenith during our observations. Several flatfields were taken using each filter. The details of the exposures are given in Table 2.

3. Data analysis and results

3.1 *Determination of the CCD Characteristics*

Two important characteristics of a CCD are its readout and spatial noise. The former determines the minimum detectable signal for situations with a small number of

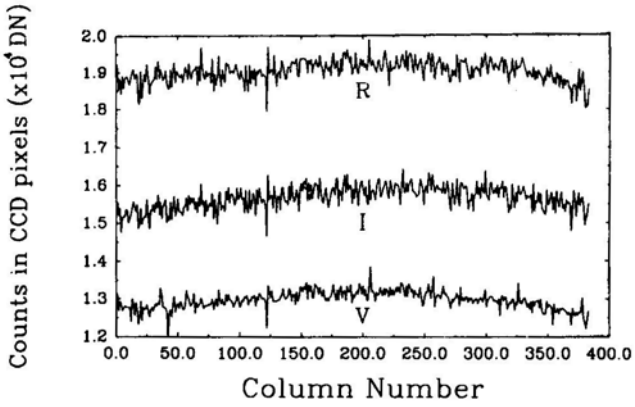

Figure 2. The typical variation of CCD pixels along a row in the centre of the chip through *V. R* and *I* filters. A bad pixel is seen at around column no. 123 showing a systematic dip in all the three filters. The rms variation in the flatfield counts along a row are less than 2% for each of the filters.

collected photons per pixel such as in spectroscopy and speckle interferometry, while the latter sets the limit for a large number of collected photons such as the detection of faint features superimposed on a night sky background. Although spatial noise can be corrected by dividing by a flatfield exposure, the variation in the quantum efficiency with wavelength from pixel to pixel is sufficiently large that differences between the spectrum of the signal and that of the flatfield become important at roughly the level of a few parts in 1000, for wavelengths near bright night sky lines (Gudehus & Hegyi 1985). Fig. 2 shows a typical variation of the counts in the CCD pixels along a central row for three different flatfields through the three filters. The root mean square fluctuations in the ADU along a typical row as shown are 1.9, 1.6 and 1.8% respectively for *V, R* and *I* flatfields.

The system gain, gain factor, or transfer factor of a CCD can be determined by studying the noise statistics of a uniform exposure or the flatfield (see e.g. Prabhu, Mayya & Anupama 1991). For a signal of N photons, the shot noise is $\sqrt{N_e}$. Since the electrons generated in a pixel are proportional to N through the scale factor of quantum efficiency of the pixel, it is generally assumed to a first degree of approximation that N_e electrons stored in a pixel have a noise component of $\sqrt{N_e}$. For a system gain of G DN/electron, the observed counts would be $S = GN_e$ and the corresponding noise $\sigma = \sqrt{N_e}$. One thus obtains $\sigma^2 = GS$, and G can be determined through the observables S and σ.

In practice the rms noise in counts is also affected by the readout noise R and the rms variations in the sensitivity of the pixels which is proportional to the signal itself. Any nonuniformity in the flatfield exposure also adds to the rms variation proportional to the signal. Thus the total variance of the counts is

$$\sigma_T^2 = G^2 R_e^2 + GS + f^2 S^2 \tag{1}$$

where f is the rms value of a normalized flatfield due to pixel-to-pixel variations and the nonuniformity of illumination of the CCD. It may appear that a least squares fit to the observed values of S and σ can yield estimates for G, R_e and f. However, since

the magnitudes of observables increase from the first term to the last term at the right hand side of Equation (1), the errors of conventional regression analysis propagate in the direction of $f_2 \rightarrow G \rightarrow G_2 R_e^2$. Horne (1988) suggests a recipe for the determination of G and R_e which was adapted here after some modifications. The following analysis were carried out using the PCVISTA software (Treffers & Richmond 1989).

Nine flatfleld images were obtained through the *I* band on January 29, 1990 with mean counts ranging from 2000 DN to 21,700 DN above bias. These were trimmed to remove the overscan area and also the first row and columns at either ends which generally showed high counts. A mean bias value was subtracted from trimmed images. The bias was estimated in three different ways:

(a) Mean of bias frames obtained before and after the series of flats;
(b) mean of row overscan region;
(c) mean of column overscan region. The difference in the different mean values was ~ 5%, and its effect on the final results is <1%.

The three flatfield exposures with highest counts were stacked to produce the master flatfield image. These images had together ~ 55000 DN per pixel implying that the field had an accuracy of ~0.4% at a system gain G ~ 1. The master flatfield was normalized to unity by dividing by the mean value over the frame. The remaining 6 flatfields were corrected using this master flatfield. A window of 100 × 200 was chosen on these frames in an area that was relatively free from defects. The remaining few defects were iteratively removed by comparing with adjacent pixels in a 5×5 window and rejecting pixels that deviated by > 3σ. The remnant rms noise was due to readout and photon statistics.

If two exposures are of similar DN, the ratios of the two will also be free of contribution to the rms by the variation due to flatfield and nonuniform illumination (Mackay 1988). One set of nearly equal flatfields was found among the six used in the above measurements, and another set was found in the three used for the master flatfield. The ratio images of these two sets were also used to obtain two more sets of estimates of noise.

3.2 *System Gain and Readout Noise*

The bias frames for this CCD used in our analyses had an rms value of 11.63 counts. Hence we added a value of variance 135 at zero signal to the set of (variance, signal) estimated from the flatfield, The resulting 9 Pairs of data were used to determine G and R using least-squares regression analysis. The SIXLIN routine developed by Isobe *et al*. (1990) was employed. The data has a regression coefficient of 0.9986.The mean of six different regression lines yields

$$\sigma^2 = (-106.85 \pm 199.14) + (0.9435 \pm 0.0267)S. \quad (2)$$

The Standard error of the fit is 337 counts. The negative value for the y-intercept implies that there is a quadratic component still present in the data. The highest point in the data will be affected the most, particularly since the two flats used in arriving at the results were dissimilar at 10% level. Deleting this last point we obtain,

$$\sigma^2 = (142.70 \pm 132.67) + (0.8876 \pm 0.0159)S. \quad (3)$$

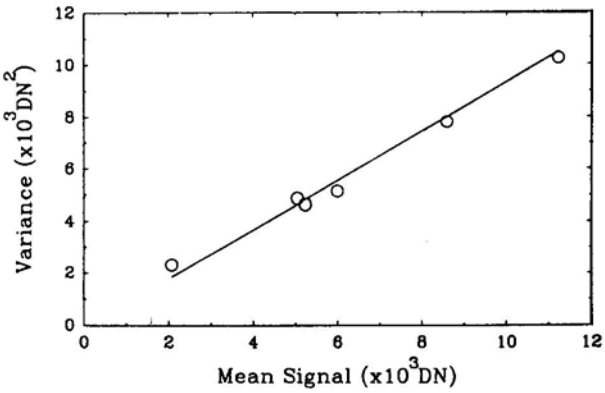

Figure 3. A plot of the total variance in units of square of ADUs as a function of the mean signal level. The data points have been computed from the flatfield frames taken with varied exposures using the *I* band filter. The straight line is a linear fit to the data points. The coefficients of the fit are used to derive the readout noise and the system gain.

The regression analysis also yields a correlation coefficient of 0.9984 and a standard error of fit 244 counts. The derived values are thus $G = 0.888 \pm 0.016$ DN per electron and $R_e = 13.5 \pm 13.0$ electrons. Fig. 3 shows a plot of σ^2 versus the mean and the regression fit to the data points.

The error on the derived value of R_e is rather high. This can be improved only by including a larger number of measurements with low values of *S.* On the other hand, the derived value is consistent with the mean value of 13.1 electrons derived from the rms of the bias frames. This value, in itself, is higher than the value specified by the manufacturers. On a closer inspection of the data, it was found that the last few bits of data had a significant probability of getting lost in the process of digitisation, possibly due to insufficient time delay between two successive data transfers. The rms of counts due to this fact had a value of 6 as seen from the flat frames. This does not have much effect at high count rates, but introduces extra noise at lower levels. Correcting the constant in the regression curve for this contribution, one obtains $R_e = 11.6$ electrons, which is only slightly higher than expected for the chip.

3.3 *Measurement of the Instrumental Magnitudes of Stars in M67*

A bias frame was subtracted from each of the observed frames. The analysis was carried out using the standard IRAF software package and the DAOPHOT (Stetson 1987) package on our SUN Sparc station. The star images were flatfielded using the twilight and the dawn sky flats. The cosmetic corrections and removal of the cosmic rays were done by applying a median filter with a 3×3 kernel. Since the CCD field is fairly crowded because of the poor seeing, we carried out the photometry of the stars in all our frames by simultaneous profile fitting using the DAOPHOT package. The relatively bright and isolated stars were used for getting the point spread function (psf) in the images. The psf radius was kept as 13 pixels and the fit radius was the

FWHM of the stars. The stars were identified using the 'daofind' program. The detection threshold was kept at 4σ counts above the sky. The sky values were determined from an annulus starting from a radius of 15 pixels and extending to a radius of 25 pixels. The measuring aperture was kept equal to FWHM of the psf (see Table 1). The minimum data value used for photometry was 3σ below the sky. The zero-point was kept equal to 23 mag for the *R* and *V* frames and 22 mag for the *I* frames. The final instrumental magnitudes r_i v_i and i_i were determined by carrying out the simultaneous psf-fitting to all the identified stars. The residual images after the removal of the simultaneously fitted stars were examined and results from badly fitted stars were ignored.

The instrumental magnitudes are then given by the following expressions.

$$v_i = -2.5\log(\mathrm{ADU}) + 23.0, \tag{4}$$

$$r_i = -2.5\log(\mathrm{ADU}) + 23.0, \tag{5}$$

$$i_i = -2.5\log(\mathrm{ADU}) + 22.0, \tag{6}$$

where ADU represents the integrated counts per sec in the psf of the star. Very bright stars that were close to saturating the CCD were ignored. An average of the magnitudes was taken where good multiple exposures were available in the same filter. These magnitudes were also used to derive the instrumental colours $(v - r)_i$ and $(r - i)_i$. The derived magnitudes and colours were then calibrated against the standard stars by carrying out regression analyses. The standard stars and their magnitudes and colours used for comparison and calibration of our CCD are listed in Table 3, and have been taken from the most recent CCD measurements by Gilliland *et al.* (1991) and Chevalier & Ilovaisky (1991). We used 15 stars with good measurements in all the three bands (and an additional one in the *V* and R only) as calibrators. Seven of these are in common with the ten calibrators used by Chevalier & Ilovaisky (1991). Three calibrators from their list had to be dropped because one (G8) was saturated, another (F81) was on the edge of the *R* frames, and third (G12) had a poor measurement. The list was, however, supplemented by additional stars from their list which had no previous record of any variability. The regression analyses were carried out for $V–v_i$ and $(v–r)_i$ as a function of *V–R* and for $(r\ \ i)_i$, $R - r_i$ and $I–i_i$, as a function of *R–I* respectively. The standard magnitudes were taken from Chevalier & Ilovaisky (1991). The linear fit was performed by the task in the STSDAS package. The points were given weights according to their measurement errors (e.g. standard deviations for *V* listed in Table 3) while deriving the best fit linear relations.

One normally images the same star at various zenith angles so that one can use the data to compute the extinction correction on the estimated magnitudes due to the atmospheric absorption of light in a given waveband. The first order atmospheric extinction corrections for the site have been measured and given in Mayya (1991). Our observations were carried out very close to the zenith (see Table 2 for air-mass). We did not apply the air-mass correction explicitly and absorbed it in our zero point correction during the regression analysis. The correction due to differences in the air-mass for different exposures in the same filter were negligible compared to the Statistical errors.

Table 3. Standard stars used for calibration.

Star No.[a]	Gilliland *et al.* (1991) V_G	$(V-R)_G$	Chevalier & Ilovaisky (1991) V_{CI}	$(V-R)_{CI}$	$(R-I)_{CI}$	Present work V	sigma	$(V-R)$	$(R-I)$
5	10.31	0.65	10.301	0.641	0.570	10.310	0.010	0.596	...
13	12.14	0.27	12.124	0.283	0.273	12.123	0.007	0.268	0.240
16	12.27	0.32	12.247	0.347	0.326	12.265	0.008	0.361	0.315
19	12.67	0.29	12.671	0.293	0.304	12.628	0.006	0.240	0.327
27	12.78	0.32	12.765	0.329	0.320	12.758	0.006	0.311	0.348
28	12.91	0.26	12.884	0.275	0.279	12.873	0.007	0.257	0.272
34	12.83	0.32	12.820	0.329	0.322	12.801	0.006	0.305	0.312
37	12.63	0.46	12.636	0.461	0.431	12.615	0.004	0.441	0.445
41	12.73	0.31	12.724	0.336	0.349	12.734	0.008	0.346	0.322
44	13.09	0.32	13.077	0.329	0.313	13.065	0.006	0.301	0.341
46	13.10	0.33	13.096	0.356	0.347	13.135	0.012	0.388	0.369
48	13.16	0.32	13.147	0.337	0.317	13.151	0.010	0.334	0.320
49	13.20	0.34	13.174	0.343	0.332	13.215	0.009	0.358	0.334
64	13.70	0.34	13.670	0.339	0.353	13.711	0.007	0.343	0.320
79.	14.14	0.42	14.132	0.416	0.382	14.186	0.010	0.436	0.372
1–49[b]			13.458	0.355	0.343	13.458	0.010	0.353	0.353

[a] Refers to numbers by Gilliland *et al.* (1991)
[b] Identification number of Eggen & Sandage (1964).

3.4 *Photometric Performance and the Colour Equations*

The regression analysis of the measured magnitudes and colours of the standards resulted in the following linear transformation equations.

$$V - v_i = (0.253 \pm 0.026)(V - R) - (0.663 \pm 0.009), \tag{7}$$

$$(v - r)_i = (0.971 \pm 0.026)(V - R) + (0.576 \pm 0.009), \tag{8}$$

$$(r - i)_i = (0.790 \pm 0.050)(R - I) + (0.616 \pm 0.017), \tag{9}$$

$$R - r_i = (0.128 \pm 0.032)(R - I) - (0.064 \pm 0.011), \tag{10}$$

$$I - i_i = (0.089 \pm 0.070)(R - I) + (0.493 \pm 0.024). \tag{11}$$

Although normally the first three relations are sufficient for data obtained with the three filters, because the CCD frames with different filters did not cover the same set of stars we derived the last two relations also so as to be applicable when only the $(r - i)_i$ colours had been measured. The data points used for the regression analysis and the resultant linear fits are shown in Fig. 4. The deviations of the measured data points around the best fit linear relations are also shown in Fig. 5. The spread in the data points represents the accuracy of the magnitude estimations using the above transformation equations. The residual rms scatter of the data points is 0.022 mag for Equations (7) and (8), 0.017 mag for Equation (9), 0.013 for Equation (10), and 0.022 for Equation (11) for the standard stars in Table 3.

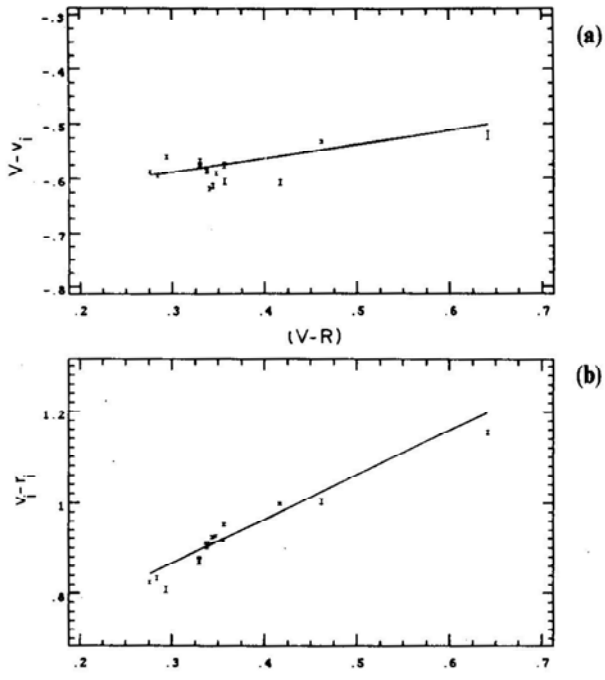

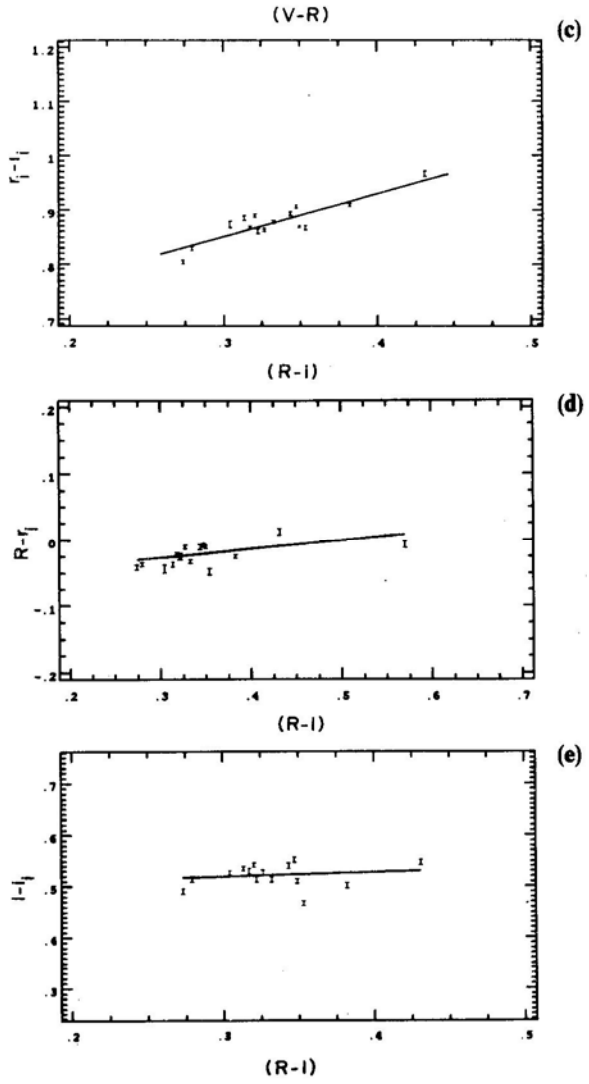

Figure 4(a–e). (**a**) Difference between the 'standard' V magnitudes published by Chevalier & Ilovaisky (1991) and our instrumental magnitudes v_i plotted as a function of the Standard colour index (V—R) for the 16 stars used as calibrators (see Table 3).The solid line represents the linear least-squares fit. Frames (**b**) through (**e**) show similar diagrams for $(v - r)_i$ and $(r - i)_i$ against (V—R) colours, and R—r_i and I — i_i against (R—I) colours, respectively.

In Table 4 we list the magnitudes and colours derived using these transformation equations for a few additional stars in M67 imaged in at least two contiguous filters. The I magnitudes have been derived using data from all three filters wherever available, else only the $(r–i)_i$ colours have been used. For comparison we also show previous measurements of these stars from the literature taken mostly from Gilliland *et al.* (1991). The stars G38 and G84 have significantly discrepant magnitudes. The V magnitude of star 38 is, however, consistent with the measurements by Racine (1971)

who also reported it to be a resolved double and somewhat blue in nature. It is probably a variable star. The *V* magnitude estimated by us for star 84 is consistent with the measurement of Chevalier & Ilovaisky (1991) who on the basis of its discrepancy with the value given by Gilliland *et al.* (1991) suspected it to be variable.

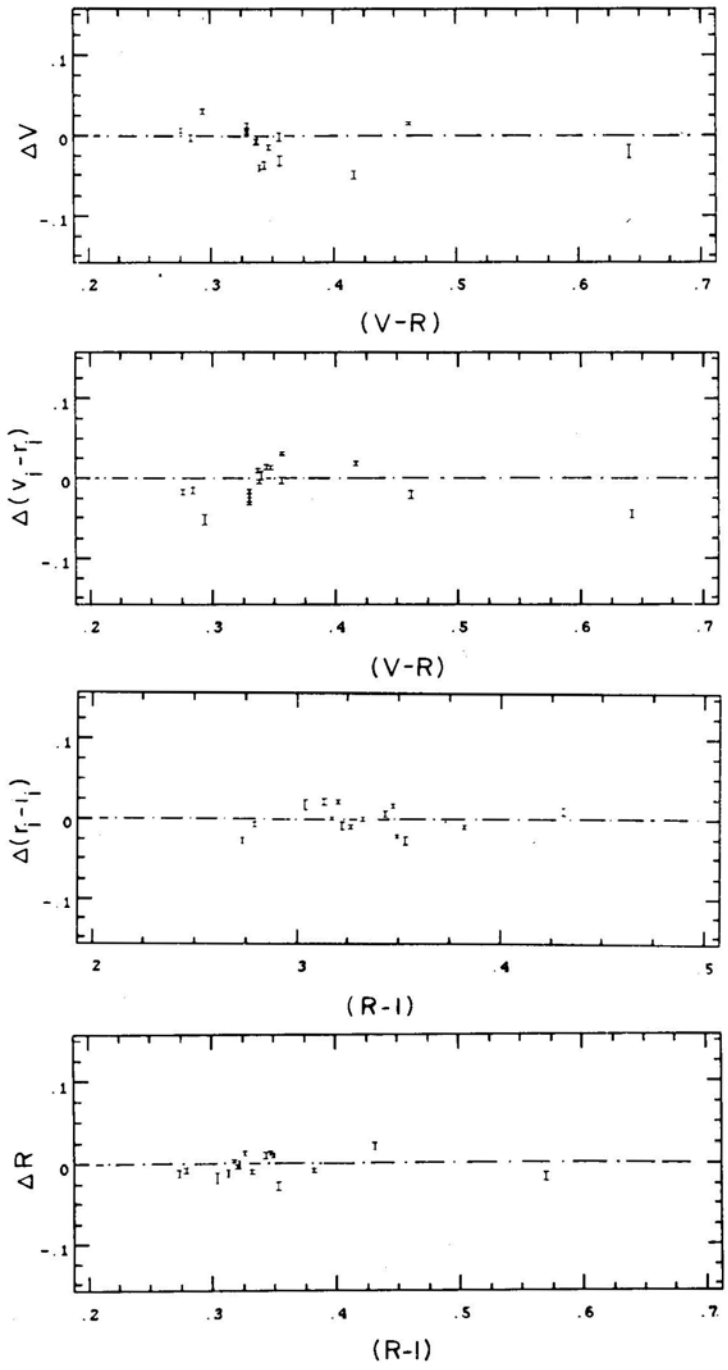

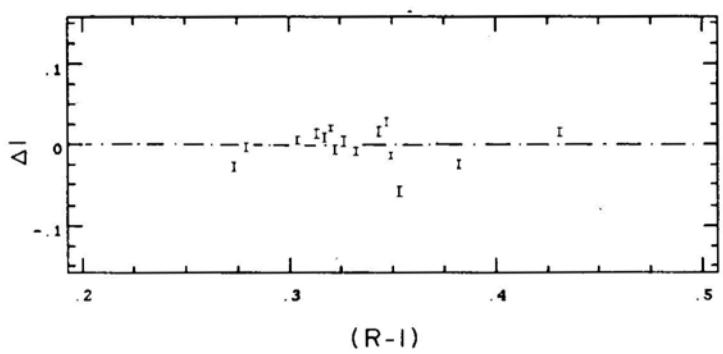

Figure 5. Residual differences between the fitted line and the data shown in Fig 4.

Table 4. Measurement parameters for stars in M67.

Star No.[a]	Previous measurement[a] V	$(V-R)$	$(R-I)$	Present work V	Sigma	$(V-R)$	$(R-I)$	R^b
17	12.40	0.42	0.441	12.408	0.008	0.448	0.359	11.96
21	12.57	0.34	0.341	...	...	...	0.315	12.20
38[c]	10.88	0.27	0.265	10.947	0.013	0.321	0.160	10.63
52	13.22	0.33	0.328	13.215	0.010	0.343	...	12.87
65	13.94	0.33	0.367	13.961	0.010	0.366	...	13.60
76	14.13	0.32	0.278	...	...	...	0.312	13.79
84	14.21	0.36	0.316	14.393	0.009	0.347	0.253	14.05

[a] Refers to numbers and measurements by Gilliland *et al.* (1991), except for *R–I* which are from Chevalier & Ilovaisky (1991).
[b] Using *R* and *I* data (See equations 10–11 in the text) where *V* data is not available.
[c] Cross-reference is *I*-242 (Joner & Taylor 1990).

4. Conclusion

CCD photometry of the stars in the 'dipper asterism' region of M67 has allowed us to obtain the colour transformation equations for the *VRI* standard bands. The typical residual rms scatter of measured quantities and therefore, the accuracy of the CCD photometry is $\simeq$ 0.02 mag for this particular CCD and filter combination used for observations in the 1990 season. The system gain is found to be 1.126 electrons per count and the readout noise is about 11.6 electrons. We conclude that stars G38 and G84 may be variable.

Acknowledgements

We would like to thank the Director of the Indian Institute of Astrophysics for allotting dark nights to us for our observations. We also appreciate the assistance rendered to us at various stages of these observations by the engineering and support the same institute.

References

Bhat, P. N., Kembhavi, A. K., Patnaik, K., Patnaik, A. R., Prabhu, T. P. 1990, *Indian J. Pure Appl. Phys.,* **28,** 649.
Chevalier, C, Ilovaisky, S. A. 1991, *Astr. Astrophys. Suppl.,* **90,** 225.
Eggen, O. J., Sandage, A. R. 1964, *Astr. J.,* **140,** 130.
Gilliland G. L., *et al.* 1991, *Astr. J.,* **101,** 541.
Gudehus D. H., Hegyi D. 1985, *Astr. J.,* **90,** 130.
Horne K. 1988, in New *Directions in Spectrophotometry,* Eds A. G. D. Phillip, D. Hayes, & S. Adelman, L. Davis Press, Schenectady, p. 285.
Howell, S. B. 1989, *Publ. astr. Soc. Pacific,* **101,** 616.
Isobe, T., Feigelson, E. D., Akritas, M. G., Babu, G. J. 1990, *Astrophys. J.*, **364,** 104.
Johnson, H. L., Sandage, A. R. 1955, *Astrophys. J.,* **121,** 616.
Joner, M. D., Taylor, B. J. 1990, *Publ. astr. Soc. Pacific,* **102,** 1004.
Mackay, C. D. 1988, *A. Rev. Astr. Astrophys.,* **24,** 255.
Mayya, Y. D. 1991, *J. Astrophys. Astr.,* **12,** 319.
Prabhu, T. P., Mayya, Y. D., Anupama, G. C. 1992, *J. Astrophys. Astr.* **13** 129.
Racine, R. 1971, *Astrophys. J.,* **168,** 393.
Ram Sagar, Pati A. K. 1990, *Bull. astr. Soc. India,* **17**, 6.
Schild R. E 1983, *Publ. astr. Soc. Pacific,* **95**, 1021.
Schild, R. E. 1985, *Publ. astr. Soc. Pacific,* **97**, 824.
Stetson, P. B. 1987, *Publ. astr. Soc. Pacific,* **99**, 191.
Treffers, R., Richmond, M. 1989, *Publ astr. Soc. Pacific,* **101,** 725.